# First-Principle-based Phonon Monte Carlo Simulation of Thermal Spreading Resistance in GaN HEMTs

Yang Shen

Department of Engineering Mechanics, School of Aerospace Engineering, Tsinghua University

January 2, 2023

# Thermal Issues in GaN HEMTs

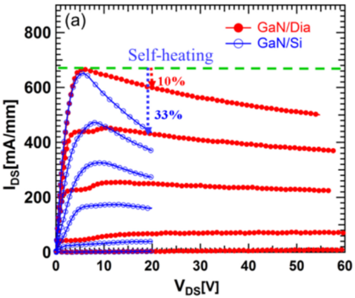


Figure 1: $I_{\mathrm{DS}} - V_{\mathrm{DS}}$ of GaN/Dia and GaN/Si HEMTs [1].

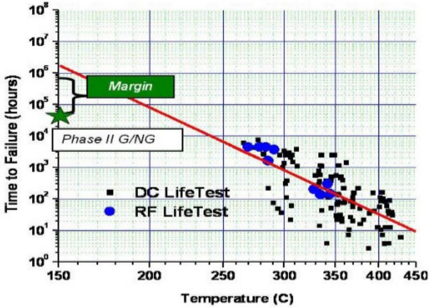


Figure 2: Mean time to failure (MTTF) for TriQuint GaN PAs [2].

The significant overheating within the device can degrade the electrical performance and shorten the device lifetime.

[1] K. Ranjan, S. Arulkumaran, G. Ng, *et al.*, "Investigation of self-heating effect on DC and RF performances in AlGaN/GaN HEMTs on CVD-diamond," *IEEE Journal of the Electron Devices Society*, vol. 7, pp. 1264–1269, 2019.

[2] M. Rosker, C. Bozada, H. Dietrich, *et al.*, "The DARPA wide band gap semiconductors for RF applications (WBGS-RF) program: Phase II results," *CS ManTech*, vol. 1, pp. 1–4, 2009.

# Thermal Spreading in GaN HEMTs

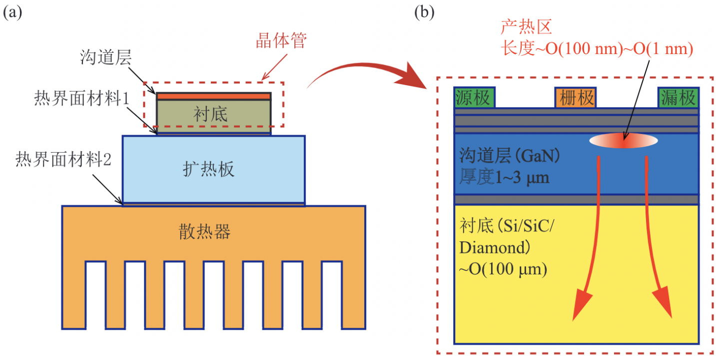


Figure 3: Schemation of the cross-section of GaN HEMTs: (a) overall structure (b) enlarged view in the near-junction region.

The size of the heat generation region is small compared with the device length and width. Thermal spreading resistance dominates the heat transport in the near-junction region.

# Phonon Ballistic Transport in the Near-Junction Region

Boundary scattering can lead to a reduced thermal conductivity, non-local transport when the heat source size comparable with MFPs can further increase hotspot temperature.

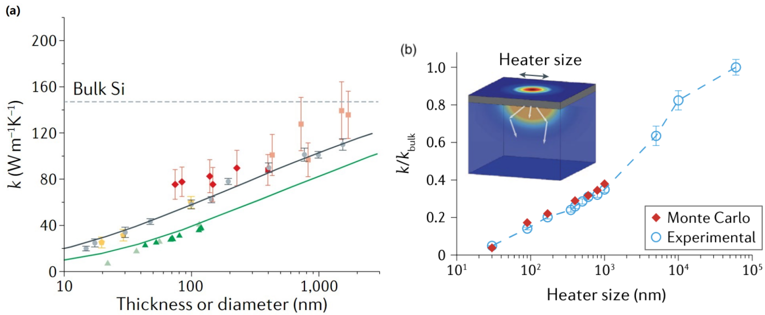


Figure 4: (a)Thermal conductivity versus film thickness or nanowire diameter. (b) Effective conductivity versus varying heater sizes[3].

[3] G. Chen, "Non-fourier phonon heat conduction at the microscale and nanoscale," *Nature Reviews Physics*, vol. 3, no. 8, pp. 555–569, 2021.

# Phonon Boltzmann Transport Equation

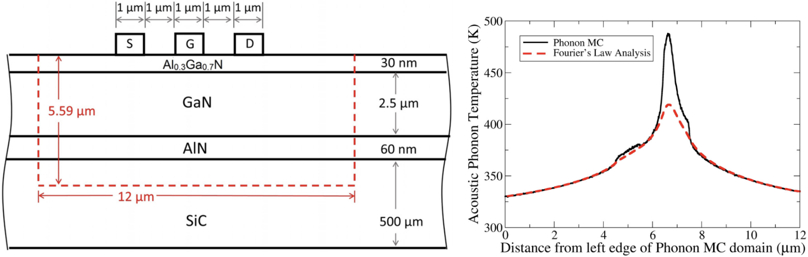


Figure 5: Schematic diagram of the cross section of the GaN HEMT and the simulated channel temperature[4].

In solving phonon BTE in the near-junction region, all previous works adopt the gray-medium approximation or empirical isotropic dispersion models.

[4] Q. Hao, H. Zhao, and Y. Xiao, "A hybrid simulation technique for electrothermal studies of two-dimensional GaN-on-SiC high electron mobility transistors," *Journal of Applied Physics*, vol. 121, no. 20, p. 204 501, 2017.

# Full-Band Phonon BTE

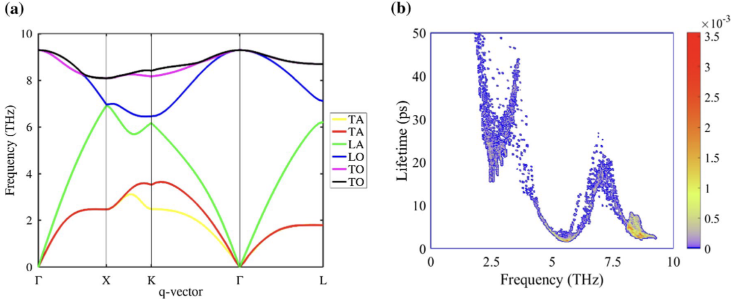


Figure 6: (a) Phonon dispersion and (b) scattering rates in cubic Ge from ab-initio calculations[5].

In theory solving the full-band phonon BTE can give most accurate temperature predictions but can be time-consuming.

[5] N. D. Le, B. Davier, N. Izitounene, *et al.*, "Study of phonon transport across si/ge interfaces using full-band phonon monte carlo simulation," *Journal of Computational Electronics*, pp. 1–12, 2022.

# This Work

- First-Principle based full-band phonon Monte Carlo simulations are conducted to investigate the near-junction thermal spreading process in GaN HEMTs.
- The reliability of isotropic empirical dispersion model and gray-medium approximation is examined.

# Phonon Dispersion and Relaxation Time

The third-order anharmonic calculation of wurtzite GaN is performed with $15 \times 15 \times 15$ **q**-point grids, generating 3375 discrete **q**-points in the reciprocal space. Since 4 atoms exist in a primitive cell, there are 3 acoustic and 9 optical phonon branches.

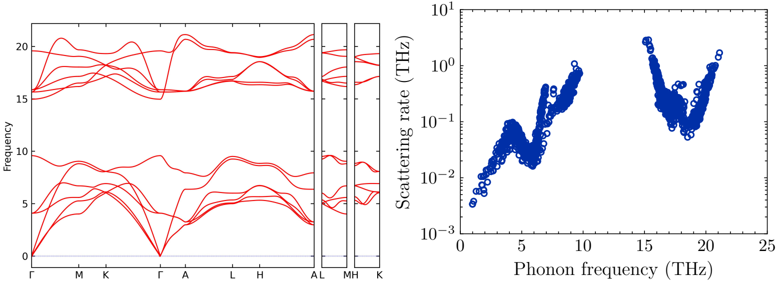


Figure 7: (a)calculated phonon dispersion along high-symmetry directions. (b) Intrinsic phonon scattring rates.

# Lattice Thermal Conductivities

Isotropic Born-von Karman dispersion:

$$\omega(k) = \omega_m \sin(\pi k / 2k_m)$$
$$\tau^{-1} = \tau_I^{-1} + \tau_U^{-1} = A\omega^4 + B\omega^2 T \exp(-C/T)$$

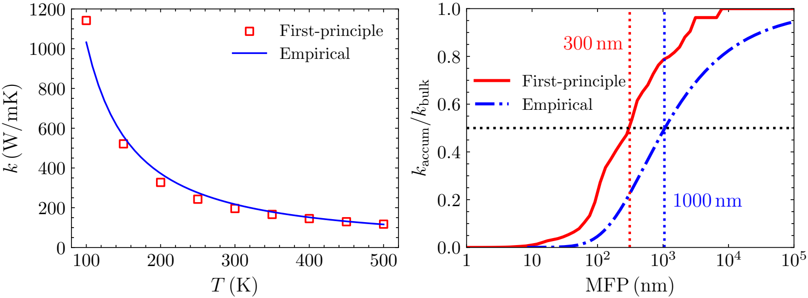


Figure 8: (a) Calculated thermal conductivity versus temperature for c axis. (b) Thermal conductivity accumulation functoin.

# Gray Medium Approximation

To well reflect the phonon ballistic effects, the average MFP can be extracted by fitting the thickness-dependent thermal conductivities:

$$\mathscr{L}\left(l_{\text{ave}}\right)=\sum_t\left|\frac{1}{3}\sum_j\int_0^{\omega_j}\frac{C_j v_{g,j} l_j}{1+\frac{4}{3}\frac{l_j}{t}}\mathrm{d}\omega-\frac{1}{1+\frac{4}{3}\frac{l_{\mathrm{avc}}}{t}}\right|^2$$

The fitted MFP of the first-principle-based predictions is 300 nm.

# Thermal Spreading Process in GaN HEMTs

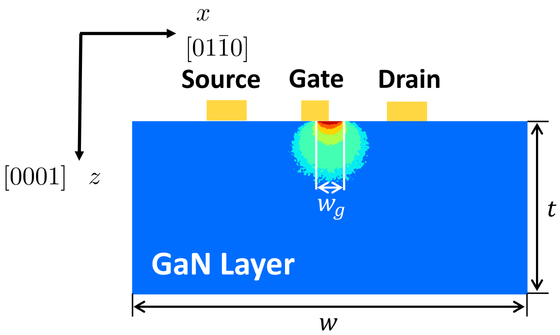


Figure 9: Schematic of thermal spreading process in the GaN layer.

# Full-Band Phonon Monte Carlo Simulation

216 irreducible points in 3375 **q**-points with 12 phonon branches.

Sample in irreducible points:

$$P_i = \sum_{j=1}^{i} \sum_{p} E_j(\omega, p) / \sum_{j=1}^{N_{ir}} \sum_{p} E_j(\omega, p)$$

Sample in phonon branches:

$$P_{i,p_j} = \sum_{k=1}^{j} E_i\left(\omega_{i,p_j}, p_j\right) / \sum_{k=1}^{12} E_i\left(\omega_{i,p_j}, p_j\right)$$

Choose the **q**-point:

$$P_{k,i,P_j} = \sum_{m=1}^{k} E_{k,i,P_j} / \sum_{m} E_{k,i,P_j}$$

# Interface Scattering

The wave-vector of reflective phonon is randomly and uniformly selected among the iso-energy states of the incident phonon:

$$P_k \propto \left(\vec{v}_k \cdot \vec{n}_\perp\right) \delta(\omega - \omega_{\text{in}}), \vec{v}_k \cdot \vec{n}_\perp > 0$$

$\Delta\omega$ chosen in this work is $\omega_m/100$.

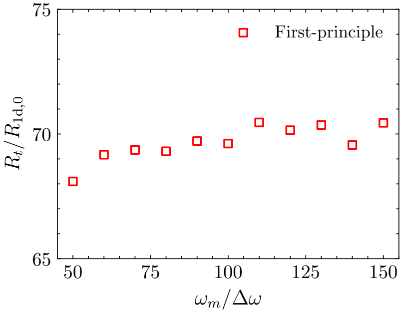


Figure 10: Dimensionless total thermal resistance calculated with different $\Delta\omega$, $t = 1\ \mu$m, $w_g/w = 0.01$, $w/t = 40$.

# Validation of the Simulation

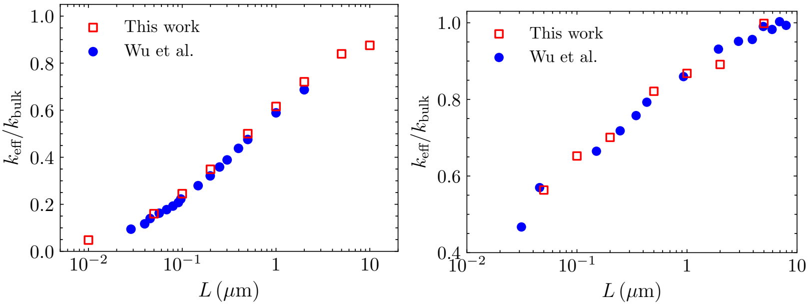


(a) Cross-plane heat conduction (b) In-plane heat conduction

Figure 11: Effective thermal conductivity varying with characteristic length in cross-plane heat conduction and in-plane heat conduction. Other numerical results come from Wu *et al.*[6]

[6] R. Wu, R. Hu, and X. Luo, "First-principle-based full-dispersion monte carlo simulation of the anisotropic phonon transport in the wurtzite gan thin film," *Journal of Applied Physics*, vol. 119, no. 14, p. 145 706, 2016.

# Thermal Spreading Resistance

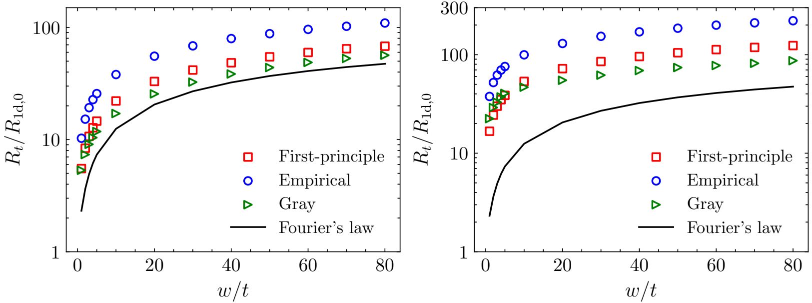


(a) $t = 3\,\mu m$ (b) $t = 0.5\,\mu m$

Figure 12: Dimensionless total thermal resistance of GaN as a function of $w/t$ with $w_g/w = 0.01$.

# Cross-Plane Ballistic Effects

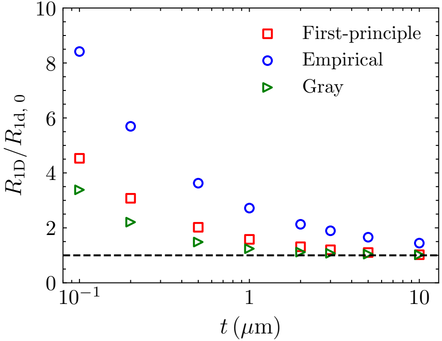


Figure 13: Dimensionless one-dimensional thermal resistance varying with layer thickness.

# Lateral Ballistic Effects

$$\frac{R_t}{R_{1d\_0}} = \frac{R_F}{R_{1d\_0}} \cdot \frac{R_{1d}}{R_{1d\_0}} \cdot \left[ \frac{R_t}{R_{1d}} \left( \frac{R_F}{R_{1d\_0}} \right)^{-1} \right]$$

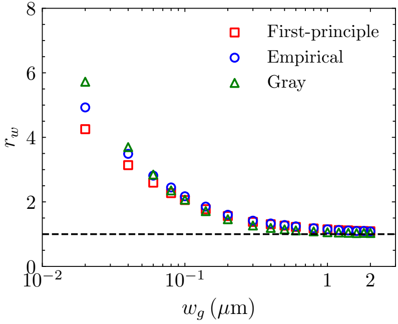


(a) $w/t = 20$

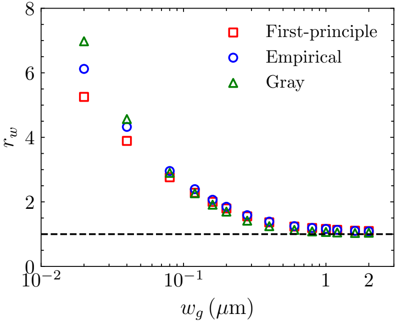


(b) $w/t = 40$

Figure 14: Thermal resistance ratio $r_w$ varying with the heat source width $w_g$, $t = 1$ µm.

# Effective Thermal Conductivity Model[7,8]

The degradation of the effective thermal conductivity is caused by the suppression of MFPs of phonons,

$$k_{\text{eff}} = \frac{1}{3}\sum_j \int_0^{\omega_j} \hbar\omega \frac{\partial f_0}{\partial T}\,\mathrm{DOS}_j(\omega) v_{g,\omega,j} l_{m,j} d\omega$$

where

$$l_{m,j} = \frac{l_{0,j}}{\left(1 + \frac{2}{3}Kn_{t\_\omega,j}\right)\left(1 + A_w\left(\frac{w_g}{w}, \frac{w}{t}\right)Kn_{w\_\omega,j}\right) r_t r_{wg}}$$

The model is developed using the empirical isotropic phonon dispersion.

[7] Y.-C. Hua, H.-L. Li, and B.-Y. Cao, "Thermal spreading resistance in ballistic-diffusive regime for gan hemts," *IEEE Transactions on Electron Devices*, vol. 66, no. 8, pp. 3296–3301, 2019.

[8] Y. Shen, Y.-C. Hua, H.-L. Li, *et al.*, "Spectral thermal spreading resistance of wide-bandgap semiconductors in ballistic-diffusive regime," *IEEE Transactions on Electron Devices*, vol. 69, no. 6, pp. 3047–3054, 2022.

# Effective Thermal Conductivity Model

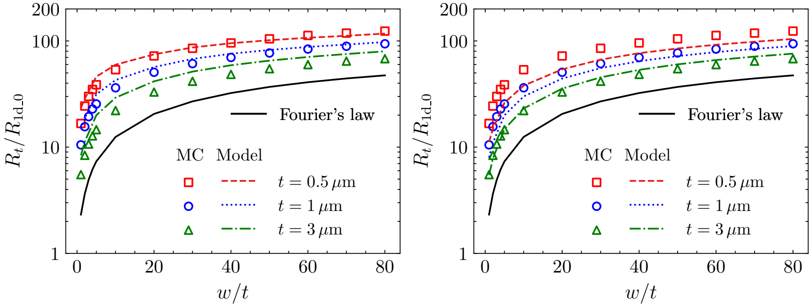


(a) $w_g/w = 0.005$

(b) $w_g/w = 0.02$

Figure 15: Dimensionless total thermal resistance of GaN as a function of $w/t$ with $w_g/w = 0.01$.

Due to the similarity of the MFP spectrum and the weak anisotropy of GaN above room temperature, the model is still valid for the first-principle-predicted phonon state properties.

# Conclusion

We develop the first-principle-driven phonon tracing Monte Carlo simulation technique to simulate the thermal spreading process in GaN HEMTs.

It is found that in predicting the thermal spreading resistance,

- The empirical isotropic model can reflect the influence of phonon MFP spectrum but overestimate phonon MFPs.
- By choosing the average MFP properly, the gray-medium approximation can approximate first-principle-based predictions roughly.
- The effective thermal conductivity model is still valid for the first-principle-predicted phonon state properties.

# Outlook

## Finished Work

- phonon dispersion
- Bias-dependent heat generation

## On-going Work

- Hybrid Monte Carlo-diffusion simulation of real GaN-on-SiC devices with full band phonon state properties and interface transmissivities

## Perspective Work

- Non-equilibrium between electrons and phonons (EMC)

*Thank You!*